Screen Printed PZT/PZT Thick Film Bimorph MEMS Cantilever Device for Vibration Energy Harvesting

R. Xu[1], A. Lei[1], C. Dahl-Petersen[1], K. Hansen[2], M. Guizzetti[2], K. Birkelund[1], E.V. Thomsen[1],O. Hansen[1,3]

[1] *Technical University of Denmark, Department of Micro and Nanotechnology, Ørsted Plads, building 345 east, 2800 Kgs. Lyngby, Denmark*
[2] *Meggitt Sensing Systems, DK-3490 Kvistgaard, Denmark*
[3] *CINF, Center for Individual Nanoparticle Functionality, Technical University of Denmark*
e-mail: Ruichao.Xu@nanotech.dtu.dk

Abstract

We present a MEMS-based PZT/PZT thick film bimorph vibration energy harvester with an integrated silicon proof mass. Most piezoelectric energy harvesting devices use a cantilever beam of a non piezoelectric material as support beneath or in-between the piezoelectric materials; it provides mechanical support but it also reduces the power output. In our device we replace the support material with another layer of the piezoelectric material. With the absence of an inactive mechanical support all stresses induced by vibrations will be harvested by the active piezoelectric elements. We show experimental results from two types PZT/PZT harvesting devices, one where the PZT thick films are high pressure treated during the fabrication and the other where the treatment is omitted. We find that with the high pressure treatment prior to PZT sintering, the films become denser and the harvester efficiency increases significantly.

Keywords: Energy harvester, MEMS, Thick film, screen printing, high pressure treatment, PZT, bimorph

1. Introduction

With the recent development in low power electronics and wireless systems it has become increasingly interesting to use energy harvesters that harness ambient energy to supply electronic sensor systems with power, and

thereby replace electrochemical batteries. The limited energy capacity of traditional electrochemical batteries makes periodical battery replacement necessary; moreover, the batteries often take up a significant volume in the total sensing system. The MEMS energy harvester addresses both issues with its large energy to volume ratio [1] and by scavenging energy from external sources. As a result, the service lifetime is only limited by material decay or fatigue. Thus the frequency of periodic maintenance may be reduced from months to years, and maybe even decades.

The most common ambient power sources are solar, thermal, mechanical or unused RF energy. Harvesting of vibration energy from a mechanical noise source can be based either on electrostatic, electromagnetic or piezoelectric conversion [2]. The interest in harvesting energy from ambient mechanical vibrations has resulted in a number of review articles in recent years [1, 2, 3, 4]. In particular the piezoelectric transduction method has received significant attention. A typical piezoelectric energy harvester is based on a bimorph cantilever beam, which consists of the active piezoelectric ceramic with metal electrodes on both sides on top of a passive mechanical support structure, which is anchored at one end and attached to a proof mass at the other [5, 6, 7, 8].

Several different piezoelectric materials are available, the materials of prime interest for application in MEMS devices, however, are PZT ($Pb(Zr_xTi_{1-x})O_3$), zinc oxide (ZnO) [9, 10] and aluminum nitride (AlN) [11, 12]. Among these, PZT is the material most commonly used in energy harvesters.

Energy harvesters using bulk PZT have been presented in [13] and [14]. These energy harvesters have large dimensions and are thus not compatible with small sensor systems. Energy harvesters made using thin film deposition methods, such as sputtering [15] or sol-gel spin-on [16, 17] are characterized by very thin PZT layers with a thickness of just a few micrometers. We wish to fabricate a PZT/PZT bimorph cantilever energy harvester, where two PZT layers are separated by a middle electrode. Here both layers are active and thus the strain energy from both layers is harvested [18]. The advantage of such a structure is that all strain energy is harvested, while in conventional structures with inactive support materials the strain energy in these is not harvested and thus wasted. Fabrication of a pure self supporting PZT beam without any mechanical support structure will be very difficult using those aforementioned thin film methods. Therefore we use thick film screen printing technique, and take advantage of the ability to screen print PZT thick films with a thicknesses of 15 μm to 60 μm to fabricate energy

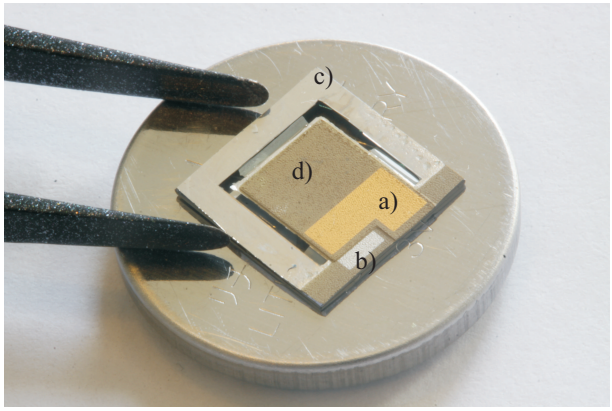

Figure 1: The bimorph MEMS energy harvester on top of a CR2032 button battery. a) The area of the Au top electrode. b) The middle electrode contact pad. c) The bottom electrode contact pad on top of the chip frame. d) The area of the the proof mass.

harvesters with a pure PZT beam [19]. With the use of PZT thick film, instead of PZT thin film, it was confirmed that a mechanical support material is indeed no longer needed in the final device, since the beam is thick and strong enough to support the proof mass.

In this work the piezoelectric PZT thick film used is InSensor®TF2100; the PZT thick films were screen printed onto the wafers then sintered. This technique has previously been used in fabrication of a piezoelectric accelerometer [20] and an energy harvester [21]. The fabricated PZT/PZT bimorph cantilever energy harvester is shown in Fig. 1.

2. Fabrication

The PZT/PZT thick film energy harvesters are fabricated using a six mask fabrication process on double sided polished 4 inch (100 mm) silicon on insulator (SOI) wafers with a 30 μm device layer, a 1 μm buried oxide layer and a 525 μm thick carrier substrate, see Fig. 2(a). The backside of the SOI wafers are patterned using UV lithography and etched using a deep reactive ion etching (DRIE) process, see Fig. 2(b). Here, the buried oxide layer is used as an etch stop layer. After an RCA clean a 1 μm thick silicon dioxide layer is grown by thermal oxidation. This layer will serve as an etch stop for a final reactive ion etch (RIE), releasing the structure, see Fig. 2(c). The bottom electrode is deposited on the front side of the SOI wafers using e-beam deposition. The bottom electrode layer consists of a

50 nm titanium adhesion layer and 500 nm of platinum which also serves as a diffusion barrier in the PZT sintering process. The bottom electrode layer is patterned using UV lithography and etched in a wet etch solution, H_2O:HCl:HNO_3 (8:7:1) at elevated temperature, see Fig. 2(d). On top of the patterned bottom electrode a PZT thick film is deposited using screen printing. Some of the wafers are subsequently high pressure treated in a process where a fluid mixture is used to apply high pressure to the wafers [19]. All wafers are then sintered, see Fig. 2(e). The Ti/Pt middle electrode is deposited through a prefabricated shadow mask using e-beam deposition, see Fig. 2(f). The shadow mask was fabricated using a 350 μm thick silicon wafer, which was patterned using UV lithography and etched through in a DRIE process. Next the second layer of PZT thick film is screen printed. The pressure treated wafers were pressure treated again, and then all wafers were sintered. The Au top electrode layer of 500 nm was also deposited through a shadow mask using e-beam deposition, see Fig. 2(g). With the two PZT stacks in place the silicon device layer was removed. First, the oxide on the backside was etched in buffered hydrofluoric acid (bHF), while the front side of the SOI wafer was protected with photoresist. The backside of the SOI wafer was finally etched in a RIE process until the device layer was removed and the cantilever released, see Fig. 2(h).

The wafer was diced and the chips polarized individually. The polarization directions of the two layers are aligned opposite to each other, i.e. during polarization the top and bottom electrodes are grounded and a polarization voltage applied to the middle electrode. The dimensions of the final energy harvester chips are shown in Table 1.

Frame Dimensions	10 mm $\times$ 10 mm
Medial dimensions	$<$ 1 mm
Cantilever width	5.5 mm
Cantilever length	1.95 mm
Mass length	4.55 mm
Total cantilever height (standard)	2 $\times$ 30 μm
Total cantilever height (high pressure treated)	2 $\times$ 20 μm

Table 1: Energy harvester dimensions.

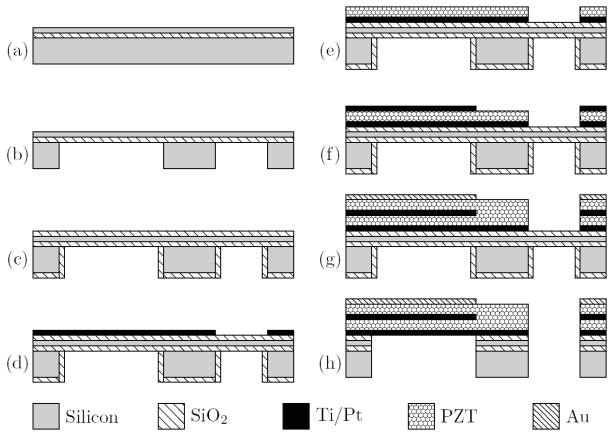

Figure 2: A cross sectional sketch of the process flow for the screen printed PZT/PZT thick film bimorph MEMS energy harvester.

3. Results

Results from two energy harvesters will be shown and discussed, harvester A is a standard harvester, while the PZT thick films on harvester B were high pressure treated before sintering. During electrical characterizations the direct and the indirect piezoelectric effect are measured. The indirect piezoelectric effect was measured using an Agilent 4294A Precision Impedance Analyzer to excite the harvester electrically, and then measure the harvester impedance magnitude and phase.

Figure 3 shows impedance measurements on harvester A, the impedance was measured between the top and bottom electrodes. The resonant frequency is $f_{\mathrm{r}} = 344$ Hz while the anti-resonant frequency is $f_{\mathrm{a}} = 347$ Hz. The impedance at resonance is the optimal resistive load, $R_{\mathrm{opt}} = 400$ kΩ. Similar measurements were done between the bottom and middle electrodes and between the middle and top electrodes. Even though the resonant and anti-resonant frequency remains the same, the optimal resistive load differ mainly due to differences in the layer thickness. The optimal resistive load between bottom and middle electrodes is $R_{\mathrm{opt}} = 180$ kΩ, while the optimal resistive load between middle and top electrodes is $R_{\mathrm{opt}} = 350$ kΩ.

The direct piezoelectric effect was measured using the aforementioned optimal resistive loads on the harvester mounted in a shaker setup. Harvester A was actuated by a B&K Mini Shaker 4810 driven by an amplified sinusoidal signal from an Agilent 33220A function generator. A B&K Piezoelectric Ac-

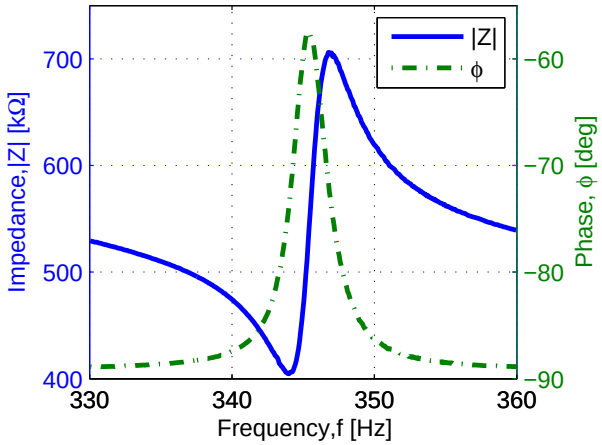

Figure 3: Impedance magnitude and phase of energy harvester A probed between the top and bottom electrodes measured at frequencies near the resonant frequency.

celerometer 8305 was mounted on the shaker along with the harvester for reference measurements. The RMS acceleration from the shaker was measured using the accelerometer and is stated in fractions of the gravitational acceleration g (9.81 m s^{-2}). Since the PZT layers are polarized in opposite directions, the power output of both layers may be measured with the top and the bottom electrodes connected by the resistive load $R_{\text{opt}} = 400$ kΩ. With the RMS voltage drop measured across the load the dissipated power can be calculated as $P_{\text{RMS}} = V_{\text{RMS}}^2/R_{\text{opt}}$. Figure 4 shows the power output as a function of the excitation frequency with acceleration as a parameter. A maximum power of 7.35 μW was measured at an acceleration of 1 g. The asymmetric shape of the power peak and the decrease in resonant frequency with increasing acceleration is probably due to a non-linear response of PZT under stress; with increasing stress in PZT the material's effective Young's modulus and the quality factor decreases [22]. The decrease in Young's modulus reduces the spring constant and thus also the resonant frequency, this is also known as a softening effect.

During measurements of the power output from the top PZT layer, the top and middle electrodes were connected by a resistive load of $R_{\text{opt}} = 350$ kΩ, while the bottom electrode was kept open circuit. In the similar measurement of the power output of the bottom PZT layer a resistive load of $R_{\text{opt}} = 180$ kΩ was used, while the top electrode was kept open circuit and results similar to those shown in Fig. 4 were obtained. The output power extracted from

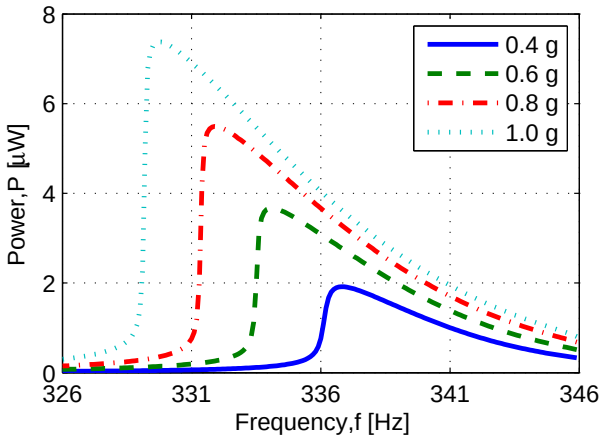

Figure 4: Power output of the energy harvester A as a function of the excitation frequency at different accelerations. The top electrode was connected to the bottom electrode through a resistive load, $R_{\text{opt}} = 400$ kΩ, optimized for maximum power using the impedance analyzer measurements.

these measurements at resonant frequency are plotted as a function of the input acceleration in Fig. 5. Figure 5 shows that the power output is indeed higher when both layers are used, but it differs from the sum of the power outputs from the two individual layers. This is probably due to mismatch between the two layers as manifested *e.g.* through the different optimal load resistances for the two layers.

The difference in optimal resistive load and power output from the bottom and the top PZT layer is caused by mismatch in PZT film thickness and material properties, which is confirmed by inspection of the cantilever cross section using scanning electron microscopy (SEM). Figure 6 shows the cross section of the PZT/PZT cantilever, and illustrates clearly the undesirable layer mismatch. Where the bottom PZT layer is thinner than the top layer, while the grains of the bottom layer appear to be larger.

The same series of measurements were also performed on the energy harvester B, *i.e.* the harvester with high pressure treated PZT thick films. The optimal resistive load for both layers combined was found to be $R_{\text{opt}} = 250$ kΩ. The output power at optimal load as a function of frequency with acceleration as a parameter is shown in Fig. 7. Table 2 shows some of the important measured results. Compared to the same measurements on harvester A, shown in Fig. 4, the power output of harvester B is significantly larger, and the softening effect is less prominent. This is evident since the

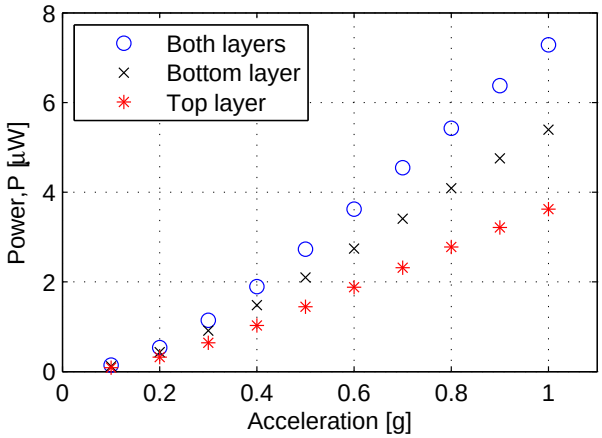

Figure 5: Power output of energy harvester A from the top PZT layer, the bottom PZT layer and both layers combined at resonant frequency as a function of the input acceleration.

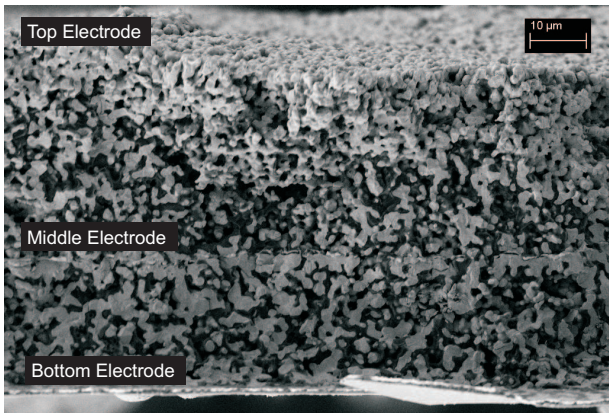

Figure 6: A SEM image showing a cross sectional view of the PZT/PZT bimorph cantilever of harvester A with PZT thick films that were not high pressure treated. The middle electrode separates the two PZT layers.

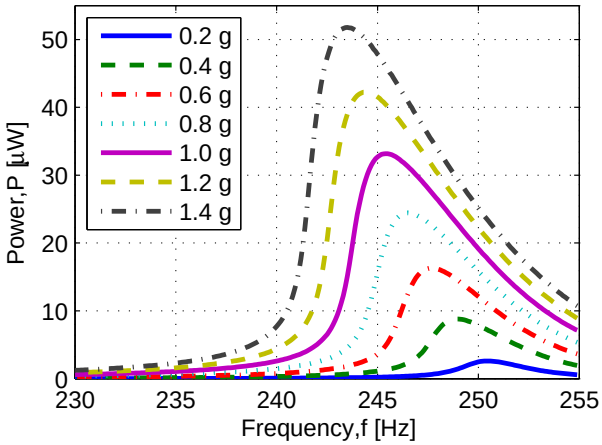

Figure 7: Power output of the energy harvester B as a function of the excitation frequency for different accelerations. The top electrode was connected to the bottom electrode through a resistive load, $R_{\text{opt}} = 250$ kΩ.

resonance peaks are more symmetric and the frequency shift as a function of input acceleration is smaller.

	Harvester A	Harvester B
Both layers		
- Power output at 1 g [μW]	7.35	33.2
- Optimal resistive load [kΩ]	400	250
Bottom layer		
- Power output at 1 g [μW]	5.39	18.9
- Optimal resistive load [kΩ]	180	150
Top layer		
- Power output at 1 g [μW]	3.62	23.6
- Optimal resistive load [kΩ]	350	180

Table 2: Summary of measured output power and optimal resistive load.

The optimal resistive load for the top PZT and the bottom PZT layers were found to be 180 kΩ and 150 kΩ, respectively. Figure 8 shows the RMS power output of harvester B across both layers, the top layer and the bottom layer as a function of the RMS acceleration. Again the power output of the two layers are not identical and the power output of both layers combined is not the sum of the powers for the two individual layers. Notice that both the

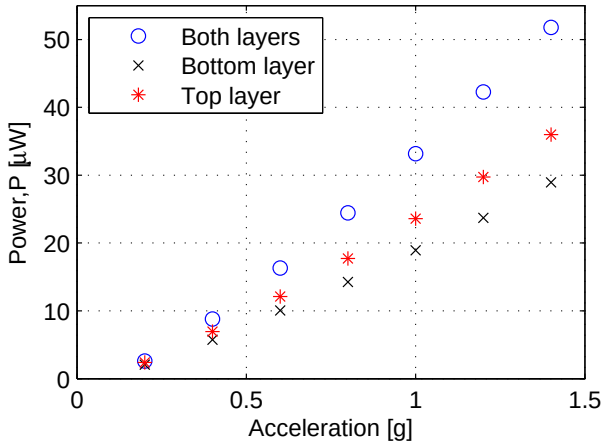

Figure 8: The power output of the energy harvester B from the top PZT layer, the bottom PZT layer and both layers at resonant frequency as a function of the input acceleration.

difference in the optimal resistive load and in output power between the two layers is now smaller compared to harvester A. The relative power output difference for harvester B at 1 g is about 20% whereas it is almost 50% for the harvester A. The difference between the two harvesters is also evident during the SEM inspection of harvester B shown in Fig. 9, where it is noted that the thickness and the grain size of the layers are now more similar than for harvester A.

In Fig. 10 the the full width at half maximum bandwidth is shown as a function of acceleration, the data were extracted from the measurements shown in Fig. 7. The increase in full width half maximum bandwidth with acceleration is a clear indication of an increased damping with increasing acceleration. The increased damping is not necessarily a drawback since the harvester becomes useful in a wider spectrum of vibrations.

4. Conclusion

Screen printed PZT/PZT thick film bimorph MEMS cantilever energy harvesters were successfully fabricated and characterized. By replacing the inactive cantilever support with another layer of PZT more power is indeed harvested than the power harvested from each individual layer. For the standard harvester at 1 g, the power output from both layers combined is 7.35 μW, while the power output for the individual layers with the same input acceleration are 5.39 μW for the bottom layer and 3.62 μW for the top

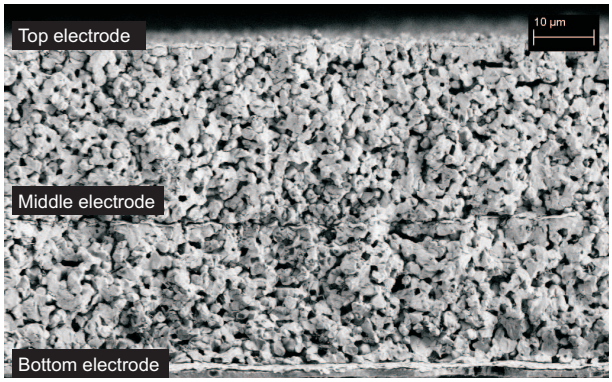

Figure 9: A SEM image showing a cross sectional view of the PZT/PZT bimorph cantilever of harvester B with PZT thick films that were high pressure treated. The middle electrode separates the two PZT layers.

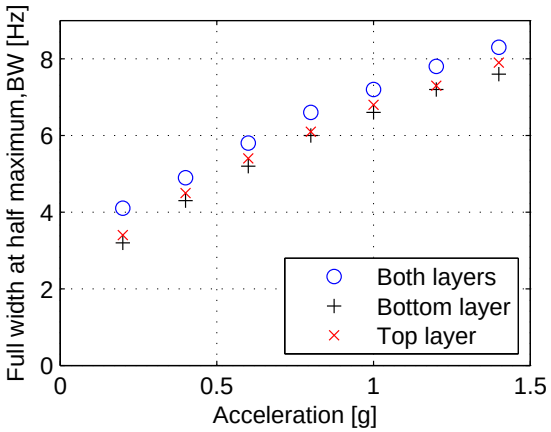

Figure 10: The full width at half maximum bandwidth for the resonance peaks of harvester B as a function of the excitation acceleration.

layer. The harvester with high pressure treated PZT thick film performed significantly better, with 33.2 μW power output from both layers combined at 1 g. The top and bottom layers have a power output at 1 g of 23.6 μW and 18.9 μW, respectively.

5. Acknowledgment

This research is part of the ELBA project, which is funded by the Advanced Technology Foundation. Center for Individual Nanoparticle Functionality (CINF) is sponsored by Danish National Research Foundation.

References

[1] N. S. Hudak, G. G. Amatucci, "Small-scale energy harvesting through thermoelectric, vibration, and radiofrequency power conversion", Journal of Applied Physics, 103, 2008.

[2] S. P. Beeby, M. J. Tudor, and N. M. White, "Energy harvesting vibration sources for Microsystems applications", Measurement Science and Technology, vol. 17, no. 12, pp. R175-R195, 2006.

[3] K. A. C.-Chennault, N. Thambi, A. M. Sastry, "Powering MEMS portable devices - a review of nonregenerative and regenerative power supply systems with special emphasis on piezoelectric energy harvesting systems", Smart Materials and Structures, vol. 17, pp. 1-33, 2008.

[4] E. Lefeuvre, A. Badel, C. Richard, L. Petit, D. Guyomar, "A comparison between several vibration powered piezoelectric generators for standalone systems", Sensors and Actuators A 126, pp. 405-416, 2006.

[5] Hua-Bin Fang et al. "Fabrication and performance of MEMS-based piezoelectric power generator for vibration energy harvesting", Microelectronics Journal, 37:1280-1284, 2006.

[6] W.J. Choi, Y. Jeon, S.G. Kim, "Energy harvesting MEMS device based on thin film piezoelectric cantilevers", Journal of Electroceramics, 17, 2006.

[7] Dongna Shen et al., "The design, fabrication and evaluation of a MEMS PZT cantilever with an integrated Si proof mass for vibration energy harvesting", Journal of Micromechanics and Microengineering, vol. 18, 2008.

[8] Swee-Leong Kok, Neil M. White, Nick R. Harris, "Fabrication and characterization of free-standing thick-film piezoelectric cantilevers for energy harvesting", Measurement Science and Technology, 20, 2009.

[9] John G. Gualtieri, John A. Kosinski, Arthur Ballato, "Piezoelectric Materials for Acoustic Wave Applications", IEEE Transactions on Ultrasonics, Ferroelectrics, and Frequency Control, Vol 41 no. 1, 1994.

[10] G. Carlotti, G. Socino, A. Petri, E. Verona, "Elastic Constants of Sputtered ZnO Films", Ultrasonics Symposium, p. 295-299, 1987.

[11] M. A. Dubois, P. Muralt, "Measurement of the effective transverse piezoelectric coefficient e_31 of AlN and $Pb(Zr_x,Ti_{x-1})O_3$ thin films", Sensors and Actuators A, Vol.77, p. 106-112, 1999.

[12] R Elfrink, T M Kamel, M Goedbloed,S Matova, D Hohlfeld, Y van Andel, R van Schaijk, "Vibration energy harvesting with aluminum nitride-based piezoelectric devices", Journal of Micromechanics and Microengineering. Vol. 19, 2009.

[13] Y. Liao, H. A. Sodano, "Model of a single mode energy harvester and properties for optimal power generation", Smart Materials and Structures, vol. 17, no. 6, p. 065026, 2008.

[14] A. Erturk, D. J. Inman, "An experimentally validated bimorph cantilever model for piezoelectric energy harvesting from base excitations," Smart Materials and Structures, vol. 18, no. 2, p. 025009, 2009.

[15] H. Jacobsen, H. Quenzer, B. Wagner, K. Ortner, and T. Jung, "Thick PZT layers deposited by gas flow sputtering", Sensors and Actuators A: Physical, vol. 135, no. 1, pp. 23-27, Mar. 2007.

[16] D. Shen et al., "Micromachined PZT cantilever based on SOI structure for low frequency vibration energy harvesting", Sensors and Actuators A: Physical, vol. 154, no. 1, pp. 103-108, Aug. 2009.

[17] H. Fang et al., "Fabrication and performance of MEMS-based piezoelectric power generator for vibration energy harvesting", Microelectronics Journal, vol. 37, no. 11, pp. 1280-1284, Nov. 2006.

[18] R.G. Ballas, "Piezoelectric Multilayer Beam Bending Actuators", Springer, 2007.

[19] C. Hindrichsen, R. Lou-Mller, K. Hansen, and E.Thomsen, "Advantages of PZT thick film for MEMS sensors", Sensors and Actuators A: Physical, vol. 163, no. 1, pp. 9 - 14, 2010.

[20] R. Lou-Moeller et al., "Screen-printed piezoceramic thick films for miniaturised devices", Journal of Electroceramics, vol. 19, no. 4, pp. 333-338, 2007.

[21] A. Lei, R. Xu, A. Thyssen, A.C. Stoot, T. L. Christiansen, K. Hansen, R. Lou-Moeller, E.V. Thomsen and K. Birkelund, "MEMS-Based Thick Film PZT Vibriational Energy Harvester", Proceeding, IEEE micro electro mechanical systems, 2011, pp. 125-128.

[22] D. Shen, J. Park, J. Ajitsaria, S. Choe, H. C. Wikle, and D. Kim, "The design, fabrication and evaluation of a MEMS PZT cantilever with an integrated Si proof mass for vibration energy harvesting", Journal of Micromechanics and Microengineering, vol. 18, no. 5, p. 055017, 2008.